

Hydrolytic Metal with a Hydrophobic Periphery: Titanium(IV) Complexes of Naphthalene-2,3-diolate and Interactions with Serum Albumin

Arthur D. Tinoco,* Emily V. Eames, Christopher D. Incarvito, and Ann M. Valentine*

Department of Chemistry, Yale University, P.O. Box 208107, New Haven, Connecticut 06520-8107

Received March 24, 2008

Serum albumin, the most abundant protein in human plasma (700 μM), binds diverse ligands at multiple sites. While studies have shown that serum albumin binds hard metals in chelate form, few have explored the trafficking of these metals by this protein. Recent work demonstrated that serum albumin may play a pivotal role in the transport and bioactivity of titanium(IV) complexes, including the anticancer drug candidate titanocene dichloride. The current work explores this interaction further by using a stable Ti(IV) complex that presents a hydrophobic surface to the protein. Ti(IV) chelation by 2,3-dihydroxynaphthalene ($\text{H}_2\text{L1}$) and 2,3-dihydroxynaphthalene-6-sulfonate ($\text{H}_2\text{L2}$) affords water soluble complexes that protect Ti(IV) from hydrolysis at pH 7.4 and bind to bovine serum albumin (BSA). The solution and solid Ti(IV) coordination chemistry were explored by aqueous spectropotentiometric titrations and X-ray crystallography, respectively, and with complementary electrochemistry, mass spectrometry, and IR and NMR spectroscopies. Four Ti(IV) species of L2 , TiL_0 , TiL_2H_0 , TiL_3H_0 , and $\text{TiL}_3\text{H}_{-1}$, adequately represent the pH-dependent speciation. The isolation of $\text{Ti}(\text{C}_{10}\text{H}_6\text{O}_2)_2 \cdot 1.75\text{H}_2\text{O}$ at pH ~ 3 and $\text{K}_2[\text{Ti}(\text{C}_{10}\text{H}_6\text{O}_2)_3] \cdot 3\text{H}_2\text{O}$ and $\text{Cs}_5[\text{Ti}(\text{C}_{10}\text{H}_5\text{O}_5\text{S})_3] \cdot 2.5\text{H}_2\text{O}$ at pH ~ 7 correlates well with the solution studies. At pH 7.4 and micromolar concentrations, the TiL_3H_0 species are favored. The $\text{Ti}(\text{naphthalene-2,3-diolate})_3^{2-}$ complex binds with moderate affinity to multiple sites of BSA. The primary site ($K = 2.05 \pm 0.34 \times 10^6 \text{ M}^{-1}$) appears to be hydrophobic as indicated by competition studies with different ligands and a hydrophilic Ti(IV) complex. The $\text{Ti}(\text{naphthalene-2,3-diolate})_3^{2-}$ interaction with the Fe(III)-binding protein human serum transferrin (HsTf), a protein also important for Ti(IV) transport, and DNA was examined. The complex does not deliver Ti(IV) to HsTf and while it does bind to DNA, no cleavage promotion activity is observed. This investigation provides insight into the use of ligands to direct metal binding at different sites of albumin, which may facilitate transport to distinct targets.

Introduction

Serum albumin (66.5 kDa) is the most abundant protein in human plasma (700 μM).¹ It displays an impressive ability to bind different classes of ligands and via this property it controls levels of many drugs and toxins.² Serum albumin also binds metal ions, predominantly soft/intermediate metal ions at one or more of at least four proposed specific sites.³ Albumin binds hard metals in chelate form.^{4–7} For example, albumin scavenges hemein, the ferric state of heme, to avoid

the formation of reactive oxygen species.⁸ Albumin binding affects the pharmacokinetics, trafficking, and efficacy of metal-based therapeutics.⁹

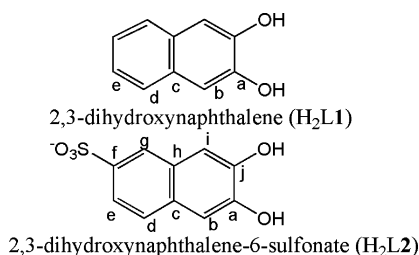
A previous study revealed that human serum albumin (HSA) binds titanium(IV) in chelate form and may transport bioactive Ti(IV) complexes.⁷ This role is more commonly associated with the Fe(III) transport protein serum transferrin

* To whom correspondence should be addressed. E-mail: atinoco9278@gmail.com (A.D.T.), ann.valentine@yale.edu (A.M.V.).

- (1) Peters, T., Jr. *All About Albumin: Biochemistry, Genetics, and Medical Applications*; Academic Press, Inc.: San Diego, 1996.
- (2) Fasano, M.; Curry, S.; Terreno, E.; Galliano, M.; Fanali, G.; Narciso, P.; Notari, S.; Ascenzi, P. *IUBMB Life* **2005**, *57*, 787–796.
- (3) Mothes, E.; Faller, P. *Biochemistry* **2007**, *46*, 2267–2274.
- (4) Larsen, S. K.; Jenkins, B. G.; Memon, N. G.; Lauffer, R. B. *Inorg. Chem.* **1990**, *29*, 1147–1152.

- (5) Caravan, P.; Cloutier, N. J.; Greenfield, M. T.; McDermid, S. A.; Dunham, S. U.; Bulte, J. W. M.; Amedio, J. C.; Looby, R. J.; Supkowski, R. M.; Horrocks, W. D.; McMurry, T. J.; Lauffer, R. B. *J. Am. Chem. Soc.* **2002**, *124*, 3152–3162.
- (6) Liboiron, B. D.; Thompson, K. H.; Hanson, G. R.; Lam, E.; Aebischer, N.; Orvig, C. *J. Am. Chem. Soc.* **2005**, *127*, 5104–5115.
- (7) Tinoco, A. D.; Eames, E. V.; Valentine, A. M. *J. Am. Chem. Soc.* **2008**, *130*, 2262–2270.
- (8) Zunszain, P. A.; Ghuman, J.; Komatsu, T.; Tsuchida, E.; Curry, S. *BMC Struct. Biol.* **2003**, *147*, 2–6807/3/6.
- (9) Thompson, K. H.; Orvig, C. *Dalton Trans.* **2006**, 761–764.

Chart 1



(80 kDa; 30 μ M) in human plasma.^{10–15} As it does with several organic ligands, HSA dramatically increases the aqueous solubility of Ti(IV) complexes well beyond their predicted solubility in plasma (pH 7.4). This behavior is particularly noteworthy with regard to stabilizing the titanocene moiety of the anticancer drug candidate titanocene dichloride,⁷ which otherwise undergoes rapid hydrolysis.¹⁶ It was postulated that by maintaining the titanocene moiety intact, serum albumin provides a mechanism by which the complex can be transported to cells and directly exhibit activity.

Studies^{4,5,8,17} on metal complex binding by HSA suggest that the location of the primary binding sites is dictated by the nature of the chelating ligands. One strategy to afford a bioactive Ti(IV) molecule might be to provide ligating groups very stabilizing of hydrolysis-prone Ti(IV) while projecting toward the biological environment a hydrophobic periphery. Investigations with a bulky, aromatic ligand that forms stable and water-soluble complexes with Ti(IV) enable characterization of the interactions crucial for the binding of such complexes to serum albumin.

For this study 2,3-dihydroxynaphthalene (H₂L1) was selected (Chart 1). Although the ligand is reasonably water soluble and readily available, few transition metal complexation studies have been performed with it. Complexes of Fe(III)/Fe(IV),¹⁸ Mo(VI),^{19,20} Pd(II),²¹ Ru(III),^{22,23} and W(VI)²⁴ have been crystallographically characterized, none of which show the metal center fully saturated by the ligand.

However, a tris(naphthalene-2,3-diolate) complex of Si(IV),^{25,26} in which the ligand fully saturates the coordination sites of the metalloid ion, has been characterized. Aqueous speciation studies on metal complexation by the derivative ligand 2,3-dihydroxynaphthalene-6-sulfonic acid (H₂L2) reveal that such ligands form high affinity complexes with strongly Lewis acidic metals.²⁷ This result augurs well for the formation of a very stable Ti(IV) complex. Some work has been performed on Ti(IV) complexation by L1 and L2.^{14,28–33} The aqueous speciation of Ti(IV) in the presence of L1 has been characterized; however, there are discrepancies in the species proposed to exist in the physiological pH range.^{28–31}

In this work, Ti(IV) complexes of L1 were synthesized and spectroscopically characterized. The aqueous speciation of Ti(IV) in the presence of L2 (owing to its better water solubility) was investigated in addition to the corresponding redox chemistry. The results are compared with the solution studies of Ti(IV) in the presence of catechol, a structurally related ligand.³⁴ Spectropotentiometric and X-ray crystallographic studies indicate that the pseudo-octahedral Ti(IV)(L1)₃²⁻ complex dominates at micromolar concentrations in the pH 7–9 range. Binding of this complex by bovine serum albumin (BSA; 75% sequence identity with HSA) was studied to determine coordination sites and affinity constants. Competition studies were performed with ligands that bind at different primary sites in serum albumin to determine the primary binding site of Ti(IV)(L1)₃²⁻. The interaction of Ti(IV)(L1)₃²⁻ with human serum transferrin (HsTf) and DNA was also examined. This investigation provides insight into specific targeting of albumin for Ti(IV) binding and delivery to respective targets and selective Ti(IV) binding at different sites of albumin depending on the chelating ligand.

Experimental Section

Materials and Instrumentation. All aqueous solutions were prepared with Nanopure-quality water (18.2 M Ω cm resistivity; Barnstead model D11931 water purifier). Human serum apotransferrin and bovine serum apo-albumin (nondefatted) were purchased from Sigma. BSA is heterogeneous depending on the fatty acid and reduced thiol content (typically \sim 0.15 SH/mol in commercial stocks.)³⁵ The purity of the proteins was checked by Coomassie-stained SDS-PAGE. Salmon sperm DNA was obtained from Sigma. Detergent compatible (DC) assay reagents were used from a Bio-Rad protein assay kit. Spectra/Por dialysis tubing

- (10) Sun, H. Z.; Li, H. Y.; Weir, R. A.; Sadler, P. J. *Angew. Chem.* **1998**, *37*, 1577–1579.
- (11) Guo, M. L.; Sun, H. Z.; McArdle, H. J.; Gambling, L.; Sadler, P. J. *Biochemistry* **2000**, *39*, 10023–10033.
- (12) Messori, L.; Orioli, P.; Banholzer, V.; Pais, I.; Zatta, P. *FEBS Lett.* **1999**, *442*, 157–161.
- (13) Tinoco, A. D.; Valentine, A. M. *J. Am. Chem. Soc.* **2005**, *127*, 11218–11219.
- (14) Tinoco, A. D.; Incarvito, C. D.; Valentine, A. M. *J. Am. Chem. Soc.* **2007**, *129*, 3444–3454.
- (15) Abeysinghe, P. M.; Harding, M. M. *Dalton Trans.* **2007**, 3474–3482.
- (16) Toney, J. H.; Marks, T. J. *J. Am. Chem. Soc.* **1985**, *107*, 947–953.
- (17) Filyasova, A. I.; Kudelina, I. A.; Feofanov, A. V. *J. Mol. Struct.* **2001**, *565*, 173–176.
- (18) Justel, T.; Muller, M.; Weyhermuller, T.; Kressl, C.; Bill, E.; Hildebrandt, P.; Lengen, M.; Grodzicki, M.; Trautwein, A. X.; Nuber, B.; Wieghardt, K. *Chem.—Eur. J.* **1999**, *5*, 793–810.
- (19) Elhendawy, A. M.; Griffith, W. P.; Omahoney, C. A.; Williams, D. J. *Polyhedron* **1989**, *8*, 519–525.
- (20) Lu, X. M.; Pei, X. H.; Wang, X. J.; Ye, C. H. *Chin. J. Chem.* **2007**, *25*, 448–452.
- (21) Okabe, N.; Hagihara, K.; Odoko, M.; Muranishi, Y. *Acta Crystallogr., Sect. C* **2004**, *60*, M150–M152.
- (22) Yang, K. Y.; Martin, J. A.; Bott, S. G.; Richmond, M. G. *Inorg. Chim. Acta* **1997**, *254*, 19–27.
- (23) Takemoto, S.; Ogura, S.; Kamikawa, K.; Matsuzaka, H. *Inorg. Chim. Acta* **2006**, *359*, 912–916.

- (24) Lu, X. M.; Wang, B.; Song, F. G.; Wang, J.; Ye, C. H. *J. Mol. Struct.* **2006**, *789*, 18–23.
- (25) Suvitha, A.; Varghese, B.; Rao, M. N. S. *Acta Crystallogr., Sect. E* **2006**, *62*, O344–O346.
- (26) Suvitha, A.; Varghese, B.; Rao, M. N. S.; Sundararajan, G.; Viswanathan, B. *Ind. J. Chem. A.* **2006**, *45*, 2193–2198.
- (27) Nakani, B. S.; Hancock, R. D. J. *Coord. Chem.* **1984**, *13*, 143–151.
- (28) Sommer, L. Z. *Anorg. Allg. Chem.* **1963**, *321*, 191–197.
- (29) Sommer, L. *Collect. Czech. Chem. Commun.* **1963**, *28*, 3057.
- (30) Tarafder, P. K.; Durani, S.; Saran, R.; Ramanaiah, G. V. *Talanta* **1994**, *41*, 1345–1351.
- (31) Mondal, R. K.; Tarafder, P. K. *Microchim. Acta* **2004**, *148*, 327–333.
- (32) Barthel, M.; Hanack, M. *J. Porphyrins Phthalocyanines* **2000**, *4*, 635–638.
- (33) Wallace, W. A.; Potvin, P. G. *Inorg. Chem.* **2007**, *46*, 9463–9472.
- (34) Borgias, B. A.; Cooper, S. R.; Koh, Y. B.; Raymond, K. N. *Inorg. Chem.* **1984**, *23*, 1009–1016.
- (35) Zhang, Y.; Wilcox, D. E. *J. Biol. Inorg. Chem.* **2002**, *7*, 327–337.

(MWCO 10 kDa) was used for dialysis. Microequilibrium dialyzers (500 μL) with ultrathin (MWCO 10 kDa) membranes were obtained from the Nest Group, Inc. $\text{H}_2\text{L1}$ and $\text{H}_2\text{L2}$ were purchased from Alfa Aesar and TCI America, respectively. Titanium and iron atomic absorption samples (both 1 mg/mL) were obtained from Aldrich and Acros, respectively. The potassium salt of titanyl bisoxalate ($\text{K}_2[\text{Ti}(\text{C}_2\text{O}_4)_2] \cdot 2\text{H}_2\text{O}$) was obtained from Gallard-Schlesinger. $\text{Na}_8[\text{Ti}(\text{citrate})_3] \cdot 6\text{H}_2\text{O}$ was prepared as described previously.⁷ Neat TiCl_4 (9.1 M) was purchased from Aldrich. Bilirubin, bromophenol blue, hemin, and ibuprofen were obtained from Sigma. All other chemicals were of high purity and used as received.

UV–vis spectra were recorded on a Cary 50 spectrophotometer (Varian). FT-IR spectra were collected on a Nicolet 6700 spectrometer using KBr pellets. Electrospray mass spectra were collected on a Waters/Micromass ZQ spectrometer at a capillary voltage of 3 kV, cone voltage of 20 V, and extractor voltage of 3 V. Fluorescence spectra were collected on a Photon Technology International QM-4 spectrofluorometer. ^1H and proton-decoupled ^{13}C NMR solution spectra were recorded on a Bruker 500 MHz instrument. CHN elemental analysis was performed by Atlantic Microlabs (Norcross, GA).

Metal Quantification. Ti(IV) content was determined by a colorimetric assay using 2,3-dihydroxynaphthalene ($\epsilon_{365} = 29\,000\ \text{M}^{-1}\ \text{cm}^{-1}$) following the procedures for the sulfonate derivative ligand.¹⁴ Fe(III) content was determined by the ferrozine assay.³⁶

pH Measurements. The pH values were determined by using a ThermoOrion Model 410 meter and an Orion 8102BNUWP electrode, calibrated with Fisher Scientific buffer solutions at pH 4, 7, and 10.

Spectropotentiometric Titrations. Carbonate-free KOH (0.1008 M) was prepared from a 1.0 M stock solution (J.T. Baker) and standardized by titration against potassium hydrogen phthalate (Mallinckrodt) using phenolphthalein (1% in 95% alcohol, Mallinckrodt) as an indicator. A solution of 0.09979 M HCl (J.T. Baker) was prepared and standardized against KOH with phenolphthalein. The stock solutions were thoroughly purged of O_2 .

The spectropotentiometric titrations were performed at 25 °C with stirring under argon. The pH was monitored as millivoltage readings by using an Orion Model 520 pH meter (accurate to 0.1 mV) and an Orion Combination pH electrode (Model 8102BNU). The electrode was calibrated before each titration by measuring voltages when aliquots of 0.1008 M KOH were added to a solution (\sim pH 2.0) prepared with 0.09979 M HCl. UV–vis spectral changes (either the growth or disappearance of ligand to metal charge transfer {LMCT} bands) due to variations in metal complexation were followed. The titration apparatus used was previously described.³⁷ UV–vis spectral data were collected (300–600 nm) by using a dip probe (0.187 cm path length) and coupler (79-100326 and 02-101593, respectively) Cary 50 accessories. All titrations were performed in the dark to prevent decomposition/oxidation of the ligands.

Complex Synthesis. Details of the syntheses and characterization of $\text{Ti}(\text{L1})_2 \cdot 1.75\text{H}_2\text{O}$, $\text{K}_2[\text{Ti}(\text{L1})_3] \cdot 3\text{H}_2\text{O}$, $(\text{Et}_4\text{N})_2[\text{Ti}(\text{L1})_3]$, and $\text{Cs}_5[\text{Ti}(\text{L2})_3] \cdot 2.5\text{H}_2\text{O}$ are given in Supporting Information.

X-ray Structure Determination. An orange block crystal of $(\text{Et}_4\text{N})_2[\text{Ti}(\text{L1})_3]$, $\text{C}_{46}\text{H}_{58}\text{N}_2\text{O}_6\text{Ti}$, having approximate dimensions of $0.20 \times 0.15 \times 0.1\ \text{mm}^3$ was mounted with epoxy cement on the tip of a fine glass fiber. All measurements were made on a Nonius

KappaCCD diffractometer with graphite monochromated Mo K α radiation. Relevant crystallographic data are presented in Table S1. For details on the data collection, refer to the Supporting Information.

Aqueous Solution Studies of Ti(IV) in the Presence of L1. A pH 7.0, 80 mL solution of 114 μM $\text{K}_2[\text{Ti}(\text{L1})_3] \cdot 3\text{H}_2\text{O}$ was prepared in water and purged with Ar. Half of the solution was titrated to pH 4.0 and the other half was titrated to pH 12.0. The UV–vis spectrum was monitored at various pH values. A complementary electrospray mass spectrometric experiment was performed with 25 mM Ti(IV) complex in 50:50 methanol/water.

Spectropotentiometric Titration of Ti(IV) in the Presence of L2. Titrations were performed on 500 μM L2 in the absence of Ti(IV) and on 167 μM $\text{Cs}_5[\text{Ti}(\text{L2})_3] \cdot 2.5\text{H}_2\text{O}$. The ligand and metal solution titrations were performed at an initial pH of 3.0 and terminated at pH 10.0. Hysteresis was checked by reverse pH titration. Initial volumes were 50 mL and all solutions contained 0.1 M KCl to maintain a minimum of a 100-fold excess of noncomplexing supporting electrolyte so that the conditional metal–ligand affinity constants are a function of concentration.³⁸ Acid and base were added by pipet followed by sufficient Ar purging.

Speciation and equilibrium constants were determined by using the SpecFit 3.0.36 global analysis system by Spectrum Software Associates that applies singular value decomposition and linear regression modeling by the Levenberg–Marquardt method to determine ligand protonation and metal–ligand binding constants. In the pH range studied, only one protonation constant of the ligand could be determined. This value in addition to the spectra corresponding to the fully protonated and monoprotonated ligand were used for the deconvolution of the metal–ligand spectropotentiometric titration data. The best fit complexation model was determined after analyzing all chemically reasonable metal–ligand species informed by the pH-dependent characterization of the Ti(IV) L2 and L1 complexes. All metal species are defined in terms of the total metal, ligand, and proton stoichiometry (MLH):



In this convention, the reacting form of the ligand is the fully deprotonated one. Protons released by hydrolysis are stipulated as negative protons because they appear as products of complexation events.

Cyclic Voltammetry. Cyclic voltammograms were measured by using a Metrohm 746 VA Trace Analyzer and a 747 VA stand. A hanging drop mercury electrode was the working electrode, Ag/AgCl/3 M KCl was the reference electrode, and a platinum wire was used as the auxiliary electrode. The potentials are reported versus NHE. All solutions were purged with N_2 . The voltammograms of 4 mM solutions of $\text{H}_2\text{L1}$ and $\text{K}_2[\text{Ti}(\text{L1})_3] \cdot 3\text{H}_2\text{O}$ were recorded at the scan rate of 25 mV s^{-1} at pH 7.0. The voltammograms of 4 mM solutions of $\text{H}_2\text{L2}$ and $\text{Cs}_5[\text{Ti}(\text{L2})_3] \cdot 2.5\text{H}_2\text{O}$ were recorded at the scan rate of 5 mV s^{-1} from pH 3.5 to 10.0. The solutions contained 0.1 M KNO_3 .

Binding Studies of Ti(IV)(L1) $_3^{2-}$ and BSA. Determination of Stoichiometry. Unless otherwise noted, all protein (and DNA) solutions were prepared/dialyzed at 25 °C in a pH 7.4 buffer that consisted of 20 mM Tris and 0.1 M NaCl.

Microdialyzers were used to study the interaction of 50 μM BSA with 1 mM $\text{Ti}(\text{L1})_3^{2-}$ in the presence and absence of 0.01% Brij (Sigma). In these dialyzers, the solutions are separated by a

(36) Tinoco, A. D.; Peterson, C. W.; Lucchese, B.; Doyle, R. P.; Valentine, A. M. *Proc. Nat. Acad. Sci. U.S.A.* **2008**, *105*, 3268–3273.

(37) Collins, J. M.; Uppal, R.; Incarvito, C. D.; Valentine, A. M. *Inorg. Chem.* **2005**, *44*, 3431–3440.

(38) Hogfeldt, E. *Stability Constants of Metal-Ion Complexes. Part A: Inorganic Ligands*; Pergamon Press: Oxford, 1982; Vol. 21.

semipermeable membrane that was previously washed with the buffer. The metal complex was determined to not bind to the walls of the dialyzers or the membrane. The solutions were shaken for 3 d at 200 rpm. The bound Ti(IV) content was then assayed as described.

A macroequilibrium dialysis experiment was performed by reacting 5–20 equiv of $\text{Ti}(\text{L1})_3^{2-}$ with 50 μM BSA and then dialyzing the reaction solution against several cycles of metal complex-free buffer over 4 d at 4 °C. The stoichiometry experiments were performed in triplicate.

Determination of Stoichiometric Binding Constants. The binding of BSA (5 μM) by various concentrations of $\text{Ti}(\text{L1})_3^{2-}$ (1–20 μM) was studied by microequilibrium dialysis. Because of the low Ti(IV) content, bound and unbound Ti(IV) concentrations were determined by the molar absorptivity of the complex at 365 nm ($\epsilon = 29\,000\ \text{M}^{-1}\ \text{cm}^{-1}$). The absorbance of the buffer solutions was subtracted from the absorbance of the protein solution. The unbound Ti(IV) content was determined by subtracting the bound content from the total added content. The solutions were equilibrated at 37 °C while being agitated at 200 rpm for 3 d. The binding constants were determined for the first three binding sites. The data were fitted applying the following equation³⁹ using Origin 7.0:

$$B = \frac{K_1L + 2K_1K_2L^2 + 3K_1K_2K_3L^3}{1 + K_1L + K_1K_2L^2 + K_1K_2K_3L^3} \quad (2)$$

where B is the binding coefficient (the concentration of bound metal complex/divided by concentration of BSA) and L is the concentration of free metal complex.

Determination of the Nature of the Primary Binding Site.

One equivalent of $\text{Ti}(\text{L1})_3^{2-}$ was incubated with 5–50 μM BSA in a competition study with 1 equiv of bilirubin, bromophenol blue, hemin, ibuprofen, or $\text{Ti}(\text{citrate})_3^{8-}$. For details of the competition study, refer to the Supporting Information.

In a separate experiment, 20 μL aliquots of BSA (107 μM) were added to a 2 mL bromophenol blue (8 μM) solution. Spectral changes of bromophenol blue due to binding to two sites in BSA was monitored by UV–vis and the corresponding affinity constant was determined using the following equation assuming identical sites:⁴⁰

$$A = [A_{\text{max}}(K_{\text{BPB}}[\text{BPB}]_0 + K_{\text{BPP}}[\text{BPP}]_0 + 1) - A_{\text{max}}(K_{\text{BPB}}[\text{BPB}]_0 + K_{\text{BPP}}[\text{BPP}]_0 + 1)^2 - (4K_{\text{BPB}}^2[\text{BPB}]_0[\text{BPP}]_0^{0.5})/2K_{\text{BPB}}[\text{BPB}]_0] \quad (3)$$

where $[\text{Ti}]_0$ and $[\text{BPB}]_0$ are the initial concentrations, BPB is bromophenol blue, and A_{max} is the maximum absorbance. A BSA sample (1.76 μM) prereacted with bromophenol blue (18.4 μM) was treated with 20 μL aliquots of 3.85 mM $\text{Ti}(\text{L1})_3^{2-}$ to measure the affinity (eq 4) of the metal complex for the bromophenol blue site using the following equation:⁴⁰

$$A = [\text{BPB}]_0(-A_0(1 + K[\text{Ti}]_0/[\text{BPB}]_0 - K[\text{BPP}]_0/[\text{A}]_0) + (A_0^2(1 + K/[\text{BPB}]_0)([\text{Ti}]_0 - [\text{BPP}]_0))^2 + 4K[\text{BPP}]_0A_0/([\text{BPB}]_0)^{0.5})/(2K[\text{BPP}]_0) \quad (4)$$

Origin 7.0 was used to fit the binding data.

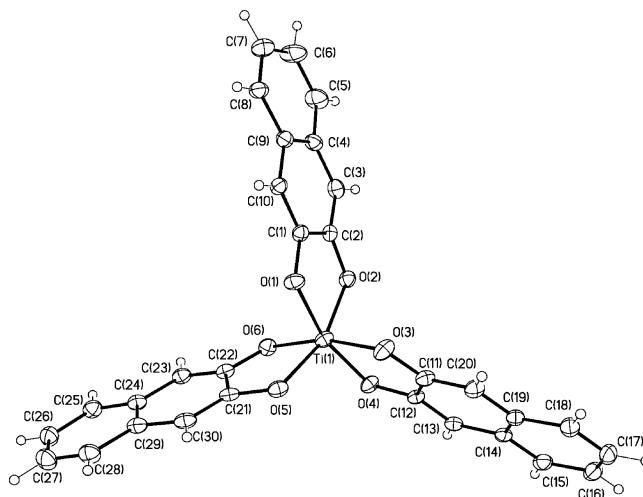


Figure 1. ORTEP diagram of $[\text{Ti}(\text{L1})_3]^{2-}$.

BSA (50 μM) was incubated with 5 equiv of $\text{Ti}(\text{L2})_3^{5-}$ for 1 d and then dialyzed extensively for 4 d in metal-free buffer at 4 °C. The Ti(IV) content in the final solution was measured.

Interaction of $\text{Ti}(\text{IV})(\text{L1})_3^{2-}$ with HsTf and DNA. HsTf (50 μM) was reacted with 5 equiv of $\text{Ti}(\text{L1})_3^{2-}$ for 1 d and then dialyzed for 4 d in metal-free buffer. The Ti(IV) content in the final solution was measured. A complementary kinetics experiment was performed under the same concentrations. The UV–vis spectrum of $\text{Ti}(\text{L1})_3^{2-}$ was followed at 365 nm to monitor dissociation of the complex in the presence and absence of HsTf at 25 °C.

Salmon sperm DNA (250 μM nucleotides) was incubated with 150 μM $\text{Ti}(\text{L1})_3^{2-}$ at 25 °C for 1 d. The UV–vis spectrum of the LMCT band $\text{Ti}(\text{L1})_3^{2-}$ (300 to 500 nm) was followed. DNA cleavage was assessed by agarose gel electrophoresis.

Results

Solid-State Characterization of Ti(IV) Complexes of L1.

Two Ti(IV) complexes of **L1** were synthesized. A 1:2 metal/ligand brown-red complex was synthesized in ethanol from the reaction of $\text{Ti}(\text{IV})(\text{aq})$ (from neat TiCl_4) with three equiv of $\text{H}_2\text{L1}$. X-ray quality crystals were not obtained but elemental analysis suggests that the formulation of the complex is $\text{Ti}(\text{L1})_2 \cdot 1.75\text{H}_2\text{O}$. It is uncertain whether the water molecules are waters of crystallization or bind to the Ti(IV). The complex is water-insoluble. The same complex can be synthesized in water under similar concentrations at pH 3.0–4.0.

A 1:3 metal/ligand orange-red complex was synthesized at pH 7.0 using KOH and recrystallized from ethanol (Supporting Information, Figure S1). Elemental analysis supports the formulation $\text{K}_2[\text{Ti}(\text{L1})_3] \cdot 3\text{H}_2\text{O}$. The tetraethylammonium salt of this complex was synthesized. The $(\text{Et}_4\text{N})_2[\text{Ti}(\text{L1})_3]$ compound crystallized in the monoclinic space group $P2_1/c$ with one molecule in the asymmetric unit and four molecules in the unit cell. The Oak Ridge Thermal Ellipsoid Plot (ORTEP) diagram for the complex is shown in Figure 1 and selected bond distances and angles are given in Table 1. The geometry about the titanium atom is pseudo-octahedral with **L1** serving as a bidentate ligand. The molecule possesses a pseudo-3-fold rotation axis perpen-

(39) Klotz, I. M. *Ligand-Receptor Energetics: A Guide for the Perplexed*; John Wiley & Sons Inc.: New York, 1997.

(40) Bertsch, M.; Mayburd, A. L.; Kassner, R. J. *Anal. Biochem.* **2003**, *313*, 187–195.

Table 1. Selected Bond Lengths (Å) and Angles (deg) for $(\text{Et}_4\text{N})_2[\text{Ti}(\text{C}_{10}\text{H}_6\text{O}_2)_3]$

Ti(1)–O(1)	1.9540(17)	O(3)–Ti(1)–O(6)	166.35(7)
Ti(1)–O(2)	1.9579(17)	O(2)–Ti(1)–O(1)	80.00(7)
Ti(1)–O(3)	1.9618(18)	O(5)–Ti(1)–O(1)	86.06(7)
Ti(1)–O(4)	1.9653(17)	O(3)–Ti(1)–O(1)	89.77(7)
Ti(1)–O(5)	1.9655(17)	O(6)–Ti(1)–O(1)	99.54(7)
Ti(1)–O(6)	1.9671(16)	O(2)–Ti(1)–O(4)	91.54(7)
		O(5)–Ti(1)–O(4)	104.73(7)
		O(3)–Ti(1)–O(4)	79.51(7)
		O(6)–Ti(1)–O(4)	93.02(7)
		O(1)–Ti(1)–O(4)	164.75(7)
O(2)–Ti(1)–O(5)	161.07(7)		
O(2)–Ti(1)–O(3)	101.86(8)		
O(5)–Ti(1)–O(3)	90.75(8)		
O(2)–Ti(1)–O(6)	89.66(7)		
O(5)–Ti(1)–O(6)	80.03(7)		

dicular to the O(1,3,5) and O(2,4,6) planes. There are no significant intermolecular contacts in the structure.

The FT-IR spectrum of $\text{Ti}(\text{L1})_2 \cdot 1.75\text{H}_2\text{O}$ and $\text{K}_2[\text{Ti}(\text{L1})_3] \cdot 3\text{H}_2\text{O}$ exhibit C=C aromatic stretches at 1507 and 1502 cm^{-1} , respectively, and C–O stretches at 1265 and 1255 cm^{-1} , respectively. These stretches are shifted to lower frequency relative to the spectrum of $\text{H}_2\text{L1}$.

Characterization of the Aqueous Speciation of Ti(IV) in the Presence of L1. A thorough aqueous spectropotentiometric titration study of Ti(IV) in the presence of L1 was hindered by the insolubility of Ti(IV) species below pH 5.5. A modified investigation of the pH speciation was performed by monitoring the UV–vis spectra of soluble species. The pH of a $\text{K}_2[\text{Ti}(\text{L1})_3] \cdot 3\text{H}_2\text{O}$ solution was adjusted from 4.0 to 12.0 under Ar. The changes of the LMCT absorbance at 365 nm were followed (Figure 2a). A fairly constant absorbance is observed in the pH range of 6.5 to 10.25, suggesting that one species dominates in this range. The UV–vis spectrum (Figure 2b) in this range is characteristic of that for the crystallized $\text{Ti}(\text{L1})_3^{2-}$ complex. The decrease in absorbance below pH 6.5 is presumed to be due to dissociation of one or two of the bound ligands because of competition with ligand protonation. Subsequent precipitation of insoluble species also accounts for the lower total absorbance. A major component of the insoluble species is

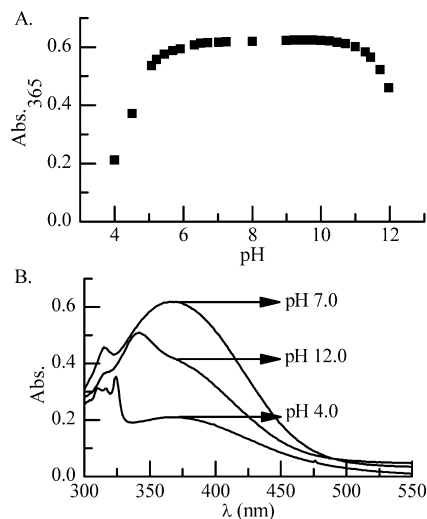


Figure 2. (A) The change in the LMCT absorbance of 114 μM Ti(IV) in the presence of 3 equiv of L1. (B) Selected UV–vis spectra at pH 4.0, 7.0, and 12.0. The path length is 0.187 cm.

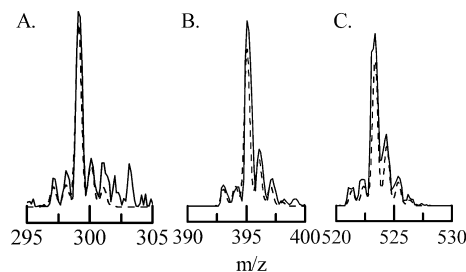


Figure 3. Electro spray mass spectra (negative ion mode) of 25 mM Ti(IV) in the presence of three equiv of L1 (50:50 methanol/water) at different pH. (A) The spectrum of the 1:1 metal:ligand complex ($\text{Ti}(\text{L1})(\text{CH}_3\text{O})_3^-$; $m/z = 299.1$) observed at pH less than 4.0. (B) The spectrum of the 1:2 complex ($\text{Ti}(\text{L1})_2(\text{CH}_3\text{O})^-$; $m/z = 395.2$) observed at pH 3.0–6.0. (C) The spectrum of the 1:3 complex ($\text{HTi}(\text{L1})_3^-$; $m/z = 523.3$) observed at pH 6.0–10.0. The theoretical spectra (dotted line) are overlaid on the experimental data (solid line).

likely the poorly soluble $\text{Ti}(\text{L1})_2$ complex. The UV–vis spectrum of this complex in ethanol shows a molar absorptivity at 376 nm that is 2/3 that of the $\text{Ti}(\text{L1})_3^{2-}$ complex ($\epsilon = 32\,000\ \text{M}^{-1}\ \text{cm}^{-1}$). The decrease in absorbance above pH 10.25 is also due to dissociation of the L1 ligands but in this range because of competition with hydroxide/oxide binding.

The electro spray mass spectra (Figure 3) of 25 mM Ti(IV) in the presence of 3 equiv of L1 also support the assertion that the 1:3 metal/ligand complex ($\text{HTi}(\text{L1})_3^-$; $m/z = 523.3$) dominates in the pH range of 6–10. The 1:2 complex ($\text{Ti}(\text{L1})_2(\text{CH}_3\text{O})^-$; $m/z = 395.2$) appears in the range 3–6. Below pH 4, the 1:1 complex ($\text{Ti}(\text{L1})(\text{CH}_3\text{O})_3^-$; $m/z = 299.1$) is present. Hydroxide or oxide bound Ti(IV) complexes of the ligand could not be detected at high pH.

The cyclic voltammogram of L1 in the range of 0.293 to $-1.5\ \text{V}$ (vs NHE) showed no redox activity at pH 7.0 (data not shown). At pH 7.0 the cyclic voltammogram of $[\text{Ti}(\text{L1})_3]^{2-}$ showed a nearly reversible redox couple with E_{red} at $-1158\ \text{mV}$ and E_{ox} at $-1086\ \text{mV}$ (Supporting Information, Figure S2). The ΔE for the system is 72 mV and the reduction potential ($E_{1/2}$) calculated is $-1122\ \text{mV}$ (vs NHE).

Chelation of Ti(IV) by L1 changes the solution spectral properties of the ligand. The fluorescence excitation spectrum ($\lambda_{\text{em}} = 410\ \text{nm}$; $\lambda_{\text{ex}} = 200\text{--}390\ \text{nm}$) of $16.7\ \mu\text{M}$ $\text{Ti}(\text{L1})_3^{2-}$ in ethanol shows a 75% quenching of the spectrum of $50\ \mu\text{M}$ L1 (Supporting Information, Figure S3). Ti(IV) complexation by L1 also affects the ^1H and ^{13}C NMR spectra. All of the proton signals of $\text{Ti}(\text{L1})_3^{2-}$ are shifted upfield with the proton at position b (Chart 1) shifting the most ($\Delta = 0.73\ \text{ppm}$). The resonances for carbons a and b are most changed by Ti(IV) chelation. The signal for carbon a is shifted downfield by 15.56 ppm whereas for carbon b it is shifted upfield by 6 ppm.

Solid-State Characterization of $\text{Cs}_5[\text{Ti}(\text{L2})_3] \cdot 2.5\text{H}_2\text{O}$. The complex $\text{Cs}_5[\text{Ti}(\text{L2})_3] \cdot 2.5\text{H}_2\text{O}$ was synthesized at pH 7.0 by ethanol precipitation of a concentrated aqueous solution of the complex. Slow vapor diffusion with ethanol yielded crystals. The connectivity was evident from X-ray crystallography but the structure could not be refined

adequately because of disorder in the position of one of the Cs⁺ counterions. Ti(IV) is bound in a pseudo-octahedral coordination environment very similar to that of Ti(L1)₃²⁻ (Supporting Information, Figure S4). Attempts to yield X-ray quality crystals by synthesizing the K⁺ or Na⁺ salts were even less successful because these salts are highly hygroscopic. The Me₄N⁺ crystalline salt cracked when removed from the mother liquor, possibly from desolvation.

The FT-IR spectrum of Cs₅[Ti(L2)₃]·2.5H₂O shows a C=C aromatic stretch at 1576 cm⁻¹ and a C–O stretch at 1256 cm⁻¹, respectively. These stretches are shifted to higher frequency relative to the spectrum of H₂L2.

Spectropotentiometric Study of Ti(IV) in the Presence of L2. pH-dependent speciation and equilibrium constants for metal–ligand complexes were determined by simultaneous fitting of UV–vis absorption spectra and pH data by using the SpecFit 3.0.36 software. The speciation was modeled for the pH range 3.0–10.0. The protonation constant of L2 was first determined and compared to literature values. A forward and backward pH titration of 500 μM L2 revealed that the titration was reversible. This issue was a concern because catechol type ligands are very susceptible to oxidation to semiquinones or quinones at high pH. The reaction system was thoroughly purged with Ar and protected from oxidation. In the pH range of study, the sulfonate moiety remains deprotonated, so the ligand is treated as an H₂L⁻ ligand. Only one of the hydroxyl protons is deprotonated in this pH range. The value of log *K* for this protonation state (HL2²⁻ + H⁺ ⇌ H₂L2⁻) was determined to be 8.11, which compares favorably with the literature value (8.09).⁴¹ The literature value for the other protonation state (L2³⁻ + H⁺ ⇌ HL2²⁻; log *K* = 12.4)⁴¹ was used for fitting purposes. The protonation constants of L2 and the spectra corresponding to the fully protonated and monoprotinated hydroxyl groups were fixed when fitting the metal–ligand speciation data.

The spectropotentiometric study of Ti(IV) in the presence of L2 was not straightforward. Attempts to perform the titration with in situ prepared solutions containing Ti(IV) and ligand in 1:3 ratio at pH 3.0 were hindered by extremely slow metal complexation kinetics, requiring hours/days of equilibration after each base aliquot addition and consequently significant solution evaporation. The equilibration of in situ prepared solutions at pH 10.0, before any pH titration was conducted, required hours. The final solution spectrum compared favorably with the pH 10.0 spectrum of a freshly prepared solution of Cs₅[Ti(L2)₃]·2.5H₂O. Therefore, the titration study was performed with solutions of Cs₅[Ti(L2)₃]·2.5H₂O, initiated at pH 10.0 and terminated at pH 3.0. Irreversible behavior occurred in the pH range of 3.0–3.5, where a yellow precipitate formed and would not redissolve as the pH was elevated. The identity of this precipitate is uncertain but it may be a polymeric species. Because a significant portion of the spectral changes that occurred during this titration appear in the pH range 3.0–5.0, data were collected in this range. Some of the analysis of

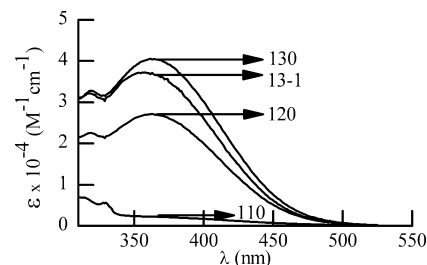


Figure 4. Molar absorptivity of the MLH 110, 120, 130, and 13-1 complexes of Ti(IV) in the presence of L2.

Table 2. Equilibrium Constants for Complexes of Ti(IV) in the Presence of L2

reaction	log <i>K</i>
TiL2 ₂ ²⁻ + L2 ³⁻ ⇌ TiL2 ₃ ⁵⁻	14.1
TiL2 ₃ ⁵⁻ + OH ⁻ ⇌ TiL2 ₃ OH ⁶⁻	3.8

these data may be limited because of the formation of this species but no data were included in which a visible precipitate was evident.

A difficulty in fitting the spectropotentiometric data was the absence of clearly defined isosbestic points to distinguish the formation and disappearance of the different Ti(IV) species (Supporting Information, Figure S5). The UV–vis data are similar to those for the nonsulfonated ligand. From pH 10.0 to 8.75, an increase in absorbance of the LMCT band is observed in addition to a shift in λ_{max} to lower energy. The absorbance remains fairly constant through pH 7.5. The absorbance decreases from pH 7.5 to 3.0. After fixing the free ligand spectral data and corresponding protonation constants, the initial model used to account for the remaining colored species included three species (MLH 110, 120, and 130 for the 1:1, 1:2, and 1:3 metal:ligand complexes). While a fit could be obtained with this model, the spectra of the calculated species did not match well with the experimental UV–vis spectra for the corollary 1:2 and 1:3 Ti(IV) complexes of L1. Significant residuals were observed for the higher pH data suggesting that hydrolyzed Ti(IV) species should be invoked. One additional species (13-1), defined in eq 5, was introduced into the model yielding a good fit to the data.



A satisfactory fit could not be obtained when trying to invoke the species 12-2 instead. The observed and calculated spectra match well for the 120 (ε₃₆₅ = 27 000 M⁻¹ cm⁻¹), 130 (ε₃₆₅ = 40 000 M⁻¹ cm⁻¹), and 13-1 species (ε₃₅₆ = 37 300 M⁻¹ cm⁻¹) (Figure 4). The spectrum for the 110 complex (ε₃₆₅ = 2,200 M⁻¹ cm⁻¹) shows a lower molar absorptivity than expected. It is uncertain whether the deconvolution of this spectrum is affected by the formation of the yellow species at the lower pH range of this titration. Equilibrium constants for the two equilibria involving the TiL₃ species that predominates near neutral pH are listed in Table 2.

The electrospray mass spectra of Ti(IV) in the presence of 3 equiv of L2 (data not shown) support the spectropotentiometric results. In the pH range 3.5–4.5, the 1:1 complex (Ti(L2)⁺; *m/z* = 285.1) and the 1:2 complex (H₂K[Ti(L2)₂]⁺; *m/z* = 563.2) are present. From pH 4.5 to

(41) Sigel, H.; Huber, P. R.; Griesser, R.; Priejs, B. *Inorg. Chem.* **1973**, *12*, 1198–1200.

10.0, the 1:3 complex ($\text{Na}_6[\text{Ti}(\text{L}2)_3]^+$; $m/z = 897.5$) is present. Hydroxide or oxide bound Ti(IV) complexes of the ligand were not detected at high pH.

The cyclic voltammogram of 4 mM **L2** in the range of 0.293 to -1.5 V (vs NHE) showed no redox activity from pH 3.5 to 10.0 (data not shown). No redox activity for the Ti(IV) complex was observed from pH 3.5 to 4.5. From pH 4.5 to 10.0 the cyclic voltammogram of 4 mM $[\text{Ti}(\text{L}2)_3]^{5-}$ showed a nearly reversible redox couple with E_{red} at -1079 mV and E_{ox} at -1007 mV (Supporting Information, Figure S6). The $[\text{Ti}(\text{L}2)_3]^{5-}$ species appears to have dominated in the pH range because of the high concentration. The ΔE for the system is 72 mV and the midpoint reduction potential ($E_{1/2}$) calculated is -1043 mV (vs NHE).

Binding Studies of Ti(IV)(L1) $_3^{2-}$ to BSA. At pH 7.4 and micromolar concentrations, the complex Ti(IV)(L1) $_3^{2-}$ dominates. The interaction of this complex with BSA was investigated by two distinct approaches. Solutions of 50 μM BSA and 1 mM $[\text{Ti}(\text{L}1)_3]^{2-}$ were incubated at 25 °C in a microequilibrium dialyzer with a 10 000 MW cutoff semi-permeable membrane separating the solutions. After 3 d of equilibration, the Ti(IV) content on both sides of the dialyzer was measured by a method involving precipitation of the protein.¹⁴ A total of 10 ± 0.5 Ti(IV) equiv were bound to the protein. The UV-vis difference spectrum of Ti(IV)-bound BSA minus the spectrum of BSA alone (data not shown) indicated that the Ti(IV) was bound as an intact $[\text{Ti}(\text{C}_{10}\text{H}_6\text{O}_2)_3]^{2-}$ complex. The molar absorptivity of the LMCT absorbance does not appear to be significantly affected by the presence of BSA. When 0.01% Brij was introduced into the solutions to suppress nonspecific binding, the amount of bound complex decreased to ~ 6 equiv. It is difficult to assess whether the decrease in the binding stoichiometry is due to elimination of nonspecific binding or a side reaction between Brij and the metal complex. A control experiment monitoring the stability of the complex in the presence of Brij revealed that the complex becomes quite unstable and an orange precipitate forms.

Separate BSA solutions were prepared that contained an excess of $[\text{Ti}(\text{L}1)_3]^{2-}$ (5–20 equiv). The solutions were equilibrated for 1 d. These samples were then extensively dialyzed in metal-complex free buffer (pH 7.4, 20 mM Tris, 0.1 M NaCl) over 4 days. The metal and protein contents were measured in the final sample. One Ti(IV) equiv (0.98 ± 0.11) remained bound to the protein. The UV-vis spectrum (data not shown) revealed that the Ti(IV) was present as an intact complex.

The $[\text{Ti}(\text{L}1)_3]^{2-}$ complex binds to several sites on BSA. Because the identity of these sites is unknown, a study was performed to determine binding constants.³⁹ Under the conditions examined, 5 μM BSA treated with 1–20 μM $[\text{Ti}(\text{L}1)_3]^{2-}$ at 37 °C, the protein was not saturated with the complex (Figure 5). The stoichiometric binding constants for the first three sites ($K_1 = (2.05 \pm 0.34) \times 10^6 \text{ M}^{-1}$; $K_2 = (1.0 \pm 0.5) \times 10^5 \text{ M}^{-1}$; and $K_3 = (3.0 \pm 1.8) \times 10^5 \text{ M}^{-1}$) were determined by applying eq 2. Fitting with two equilibrium constants does not yield a satisfactory fit.

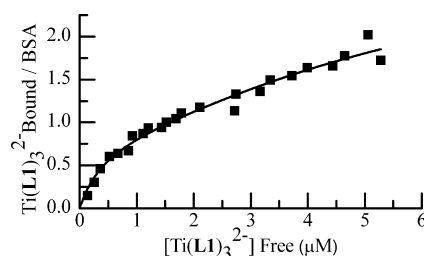


Figure 5. Equilibrium dialysis determination of the stoichiometric binding constants of the interaction of $[\text{Ti}(\text{L}1)_3]^{2-}$ with 5 μM BSA at pH 7.4 and 37 °C. The fit is superimposed on the data.

Determination of the Nature of the BSA Primary Binding Site for $[\text{Ti}(\text{L}1)_3]^{2-}$. Ligand competition experiments were performed at 25 °C to identify the BSA primary binding site for $[\text{Ti}(\text{L}1)_3]^{2-}$. The HSA ligands bilirubin (subdomain IIB; $K = 9.5 \times 10^7 \text{ M}^{-1}$),¹ bromophenol blue (drug site 1; $K = 1.5 \times 10^6 \text{ M}^{-1}$),¹ hemin (subdomain IB; $K = 1 \times 10^8 \text{ M}^{-1}$),⁸ ibuprofen (drug site 2; $2.7 \times 10^6 \text{ M}^{-1}$),¹ and $\text{Ti}(\text{citrate})_3^{8-}$ (which binds as $\text{Ti}(\text{citrate})$ to an undetermined site)⁷ were selected for this study because they bind to different primary sites in HSA (Supporting Information, Figure S7), and likely to similar sites in BSA. One equivalent of $[\text{Ti}(\text{L}1)_3]^{2-}$ was incubated with 5–50 μM BSA in the presence of 1 equiv of each of the ligands in separate solutions. The protein samples were then dialyzed to remove unbound small molecules. The bound Ti(IV) content and bound ligand content were determined. In all of the experiments, 1 equiv of $[\text{Ti}(\text{L}1)_3]^{2-}$ remained bound to BSA even when 1 equiv of the ligands was still bound. The presence of $[\text{Ti}(\text{L}1)_3]^{2-}$ in the protein sample following dialysis suggests that it is located in its primary binding site.

A further competition study was performed between $[\text{Ti}(\text{L}1)_3]^{2-}$ and bromophenol blue for BSA binding at 25 °C. Bromophenol blue binds to hydrophobic sites of BSA.⁴⁰ The absorption spectrum of the ligand is quite sensitive to binding to its primary two sites in BSA.⁴⁰ A UV-vis spectral titration was performed to quantify the affinity of bromophenol blue for these two presumably very similar sites in BSA following a literature protocol.⁴⁰ Aliquots of BSA were added to a bromophenol blue solution. The λ_{max} of bromophenol blue is red-shifted from 590 to 620 nm, and the total molar absorptivity decreases when it binds to BSA. The absorbance difference at 620 nm was plotted versus BSA concentration and fitted to eq. 3 (Supporting Information, Figure S8). The binding constant was determined to be $K_{\text{BPB}} = (5.6 \pm 0.6) \times 10^4 \text{ M}^{-1}$. The affinity of $[\text{Ti}(\text{L}1)_3]^{2-}$ for these hydrophobic sites was determined by following the disappearance of the absorbance at 620 nm (Figure 6) as aliquots of $[\text{Ti}(\text{L}1)_3]^{2-}$ were titrated into a BSA sample preequilibrated with bromophenol blue. The data were fitted to eq 4 yielding the relative binding constant $K = 0.37 \pm 0.3$. The affinity of $[\text{Ti}(\text{L}1)_3]^{2-}$ for these sites can be obtained by applying the following equation:

$$K = K_{\text{Ti}}/K_{\text{BPB}} \quad (6)$$

K_{Ti} was determined to be $2.07 \times 10^4 \text{ M}^{-1}$.

The binding interaction of $[\text{Ti}(\text{L}2)_3]^{5-}$ with BSA was also briefly investigated. BSA (50 μM) was treated with 5 equiv

of $\text{Ti}(\text{L2})_3^{5-}$ and then dialyzed extensively in metal-free buffer. The complex, like $\text{Ti}(\text{L1})_3^{2-}$, binds intact to BSA. Under the reaction conditions, 0.22 equiv of the complex bind to the protein.

Interaction of $\text{Ti}(\text{IV})(\text{L1})_3^{2-}$ with HsTf and DNA. The UV-vis spectrum of 50 μM HsTf (data not shown) obtained following the reaction with 5 equiv of $\text{Ti}(\text{L1})_3^{2-}$ and subsequent dialysis in metal-free buffer did not show the signature LMCT spectrum at 321 nm for $\text{Ti}(\text{IV})$ bound to the tyrosines of the specific metal binding sites.^{10,11,14} nor that the complex was bound intact to the protein. The corollary kinetics experiment performed under the same conditions (without the dialysis step) also showed that $\text{Ti}(\text{IV})$ was not delivered to the protein. Any $\text{Ti}(\text{IV})$ complex dissociation that was evident was also observed in the protein-free control solutions by UV-vis spectroscopy.

The UV-vis spectrum of 150 μM $\text{Ti}(\text{L1})_3^{2-}$ is unchanged when the metal complex is reacted with salmon sperm DNA (250 μM nucleotides). The complex does appear to bind to DNA as suggested by the persistence of the complex detected by the UV-vis spectrum of a dialyzed sample (data not shown). The absence of both binding-induced hypochromism and λ_{max} increase in the UV-vis spectrum suggest that DNA intercalation is not occurring.⁴² An agarose gel (Supporting Information, Figure S9) was run of DNA untreated or treated with $\text{Ti}(\text{L1})_3^{2-}$ for 24 h. The profiles of the two corresponding lanes are the same, suggesting that the complex does not hydrolyze DNA.

Discussion

Characterization of the Solid-State $\text{Ti}(\text{IV})$ Complexation by L1 and L2 . Although a 1:1 metal/ligand complex was not synthesized in this work, several multinuclear $\text{Ti}(\text{IV})$ complexes were previously crystallized with L1 , featuring essentially 1:1 stoichiometry.³³ Two $\text{Ti}(\text{IV})$ complexes of L1 were synthesized in this study from aqueous solution at distinct pH values. At pH 3.0, the neutral complex $\text{Ti}(\text{L1})_2 \cdot 1.75\text{H}_2\text{O}$ was synthesized. It is water insoluble and only moderately soluble in alcohols. It is unclear whether the water molecules, written as hydrates, are bound in some mode to the $\text{Ti}(\text{IV})$ center as no X-ray quality crystals were grown. It is very likely that the water molecules bind the metal center resulting in a hexacoordinate structure. No evidence for a dimer or higher oligomer was obtained by mass spectrometry. Two other 1:2 metal/ligand complexes have been synthesized, $\text{WO}_2(\text{L1})_2^{2-}$ and $\text{MoO}_2(\text{L1})_2^{2-}$.^{19,20,24} These complexes exhibit hexacoordinate structures. The presence of the dioxo ligands is suggestive of a hydrolysis state that would better mimic potential $\text{Ti}(\text{IV})$ L1 complexes that might form at high pH.

At pH 7.0, the complex $\text{K}_2[\text{Ti}(\text{L1})_3] \cdot 3\text{H}_2\text{O}$ was synthesized. It is reasonably water soluble. An X-ray crystal structure was obtained of the tetraethylammonium salt, which shows the L1 ligand coordinated in a typical κ^2 -diaryloxo fashion instead of the unusual η^6 -arene mode, as has been observed for $\text{Ru}(\text{III})$.²³ Currently, no other comparable

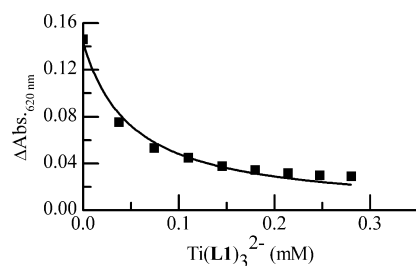


Figure 6. UV-vis difference titration of aliquots of 3.85 mM $\text{Ti}(\text{L1})_3^{2-}$ into a BSA sample (1.76 μM) preequilibrated with bromophenol blue (18.4 μM). The fit (solid line) is overlaid on the data (■).

transition metal tris(L1) complex has been isolated. A tris(L1) complex of $\text{Si}(\text{IV})$ was crystallographically characterized.²⁶ Despite both $\text{Si}(\text{IV})$ and $\text{Ti}(\text{IV})$ structures being hexacoordinate, there are important differences. The average M–O bond length is 1.785 Å and 1.962 Å for $\text{Si}(\text{IV})$ ²⁶ and $\text{Ti}(\text{IV})$, respectively. The average O–M–O angle for cis oxygens of the same ligand is 87.5° for $\text{Si}(\text{IV})$ and 79.8° for $\text{Ti}(\text{IV})$. The average O–M–O angle for trans oxygens is 175.1° for $\text{Si}(\text{IV})$ and 164.1° for $\text{Ti}(\text{IV})$. The $\text{Ti}(\text{IV})$ structure is clearly more distorted from ideal octahedral geometry. Differences in the ionic radius of the two metal ions probably most contribute to this finding. The ionic radius for 6-coordinate, octahedral $\text{Si}(\text{IV})$ is 0.4 Å and for $\text{Ti}(\text{IV})$ is 0.605 Å.⁴³ The smaller size of $\text{Si}(\text{IV})$ facilitates chelation of L1 in a more idealized geometry. The structure of $\text{Ti}(\text{L1})_3^{2-}$ compares quite favorably with the structure of $\text{Ti}(\text{catecholate})_3^{2-}$.³⁴ This observation is not surprising considering how similar catechol and L1 are. The average Ti–O bond length in the catecholate structure is 1.956 Å. The average O–Ti–O angle for cis oxygens of the same ring is 80.3°. The average O–Ti–O angle for trans oxygens is 166.3°.

The ligand L2 appears to form the same type of $\text{Ti}(\text{IV})$ complexes as does L1 over similar pH ranges. The complex $\text{Cs}_5[\text{Ti}(\text{L2})_3] \cdot 2.5 \text{H}_2\text{O}$ was isolated from a pH 7.0 aqueous solution. A preliminary crystallographic structural analysis of the complex suggests that the structure is comparably distorted from idealized octahedral geometry as $\text{K}_2[\text{Ti}(\text{L1})_3] \cdot 3\text{H}_2\text{O}$. However, the counterions in the structure are disordered and preclude satisfactory minimization.

Characterization of the pH Aqueous Speciation of $\text{Ti}(\text{IV})$ in the Presence of L1 and L2 . Limited characterization could be performed of the aqueous speciation of $\text{Ti}(\text{IV}) \cdot \text{L1}$ because of insolubility of the ligand and some of its complexes. Below pH 5.5 at the concentrations studied, some $\text{Ti}(\text{IV})$ species precipitated from solution. Even after adding <5% of a cosolvent such as ethanol or acetonitrile, these species remained fairly insoluble. Synthetic and electrospray mass spectrometric studies suggested that the dominant insoluble species is a 1:2 metal/ligand neutral complex. The solubility of a potential 1:1 complex could not be examined because such a species was not isolated from solution. Above pH 5.5, a 1:3 complex appears to dominate. A stable UV-vis spectrum was observed for ~100–200 μM solutions of $\text{Ti}(\text{L1})_3^{2-}$. This complex was crystallographically characterized as described above. At pH

(42) Long, E. C.; Barton, J. K. *Acc. Chem. Res.* **1990**, *23*, 271–273.

(43) Shannon, R. D. *Acta Crystallogr., Sect. A* **1976**, *32*, 751–767.

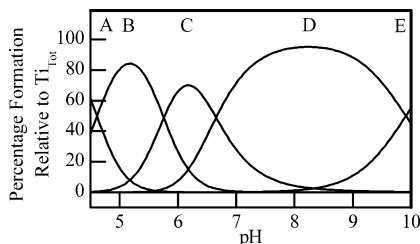


Figure 7. pH speciation diagram for 167 μM Ti(IV) in the presence of **L2** in a 1:3 molar ratio. The species depicted are (A) Ti(IV)(aq) and hydrolyzed species thereof, (B) TiLH_0 , (C) TiL_2H_0 , (D) TiL_3H_0 , and (E) $\text{TiL}_3\text{H}_{-1}$.

values higher than 10, Ti(IV) hydrolysis occurs resulting in the decrease of the LMCT absorbance and shift in λ_{max} to lower wavelength. However, the Ti(IV) remains quite soluble under these conditions. The aqueous solution behavior of $\text{Ti}(\text{L1})_3^{2-}$ compares favorably with that of $\text{Ti}(\text{catecholate})_3^{2-}$.³⁴ Ti(IV) remains coordinatively saturated by catecholate at similar concentrations through at least pH 10. Ti(IV) hydrolysis then occurs above this pH leading to the formation of a $[\text{TiO}(\text{catecholate})_2]_2^{4-}$ species. The very similar decrease in the LMCT absorbance and shift in λ_{max} to lower wavelength at high pH for solutions of $\text{Ti}(\text{catecholate})_3^{2-}$ because of the formation of the hydrolyzed species suggest that a similar 12-2 Ti(IV) **L1** species may form above pH 10.

The reduction potential of $\text{Ti}(\text{L1})_3^{2-}$ is -1122 mV (vs NHE). This value is very similar to that of $\text{Ti}(\text{catecholate})_3^{2-}$ (-1140 mV).³⁴ These values are extremely negative suggesting that these complexes would not be reduced by any biological reducing agent such as NADPH,⁴⁴ glutathione,⁴⁴ or DTT.⁴⁵ Compared to the standard reduction potential for unligated Ti(IV), $\text{H}_2\text{L1}$ greatly stabilizes the +4 oxidation state, shifting the potential by nearly a volt.³⁴

Aqueous spectropotentiometric studies of Ti(IV) in the presence of the more soluble ligand **L2** were performed to model the speciation of Ti(IV) with **L1**. The presence of the sulfonate moiety not only increases the aqueous solubility of the ligand but also increases the solubility of its Ti(IV) complexes. The spectral and potentiometric data were fit with SpecFit 3.0.36 after fixing the corresponding data for the ligand alone titration. The model that best fit the data included the species MLH_0 , ML_2H_0 , ML_3H_0 , and ML_3H_{-1} . Only the spectrum predicted for the MLH_0 species is unsatisfying and may be the result of insufficient deconvolution of the spectral data for this species. A yellow, insoluble species, that could be a polymeric version of the 1:1 metal/ligand complex, forms at the low end of the pH range where the MLH_0 species is believed to be detected. Several multimeric, partially hydrolyzed 1:1 Ti(IV) complexes of **L1** have been observed to be yellow precipitates.³³ At 167 μM , the model predicts the species distribution presented in Figure 7. From pH 4.5 to 7.0, the MLH_0 and ML_2H_0 species are present. From pH 7.0 to 10.0, the ML_3H_0 species dominates. At higher pH, the species ML_3H_{-1} becomes prevalent, which

was not observed for the catechol ligand.³⁴ The species ML_2H_{-2} that was speculated to exist in the **L1** system was not observed in the experimental pH range for **L2**. The species ML_3H_{-1} most likely converts to ML_2H_{-2} at higher pH.

It is difficult to compare the equilibrium constant values determined for the Ti(IV) **L2** system with those obtained by an earlier study²⁹ because in that work many species, including the free Ti(IV) ion, are formulated as titanil species. It is highly debated whether titanil species exist at low pH.⁴⁶ In the earlier work, the species $\text{MO}(\text{HL})_2$, MOL_2 , MOL_3 , and ML_3 (using the author's method of elemental formulation) are proposed.²⁹ Likewise, comparisons with Ti(IV) catecholate speciation work are difficult because of the implication of titanil species as the Ti(IV) source.⁴⁷ The speciation model proposed in this work is similar to the Fe(III) case for **L2**.⁴⁸ In the Fe(III) study, the species MLH_0 ($\log K_1 = 19.9$), ML_2H_0 ($\log K_2 = 14.5$), and ML_3H_0 ($\log K_3 = 9.8$) are postulated with sequential equilibrium constants comparable to the Ti(IV) case.

The reduction potential of $\text{Ti}(\text{L2})_3^{5-}$ was determined to be -1043 mV (vs NHE). This value is less negative than the value measured for $\text{Ti}(\text{L1})_3^{2-}$. To an extent, reduction potentials are correlated with affinity constants.³⁴ This correlation implies that the overall affinity of $\text{Ti}(\text{L2})_3^{5-}$ for Ti(IV) relative to Ti(III) is weaker than $\text{Ti}(\text{L1})_3^{2-}$. The aqueous speciation studies lend support to this conclusion. The UV-vis spectrum for $\text{Ti}(\text{L1})_3^{2-}$ is stable over a larger and slightly higher pH range than for $\text{Ti}(\text{L2})_3^{5-}$. The sulfonate moiety in **L2** draws electron density away from the oxygen binding atoms and thus weakens their affinity for Ti(IV). Overall, however, the pH speciation in the presence of **L2** models well the speciation in the presence of **L1**.

Specific Binding of Ti(IV)(L1)₃²⁻ to BSA. At pH 7.4 and at micromolar concentrations, $\text{Ti}(\text{IV})(\text{L1})_3^{2-}$ dominates in solution. As with the titanocene and Ti(citrate) complexes previously studied,⁷ serum albumin binds $\text{Ti}(\text{IV})(\text{L1})_3^{2-}$ as an intact complex. This result further supports the implication of albumin as an excellent reservoir for soluble Ti(IV).

The $\text{Ti}(\text{L1})_3^{2-}$ complex was selected for studying potential hydrophobic interactions with BSA. Equilibrium dialysis studies reveal that at least 10 equiv of the complex bind to the protein at different types of sites. High-stoichiometry binding to albumin is a property observed for numerous ligands.^{1,39} Most of this binding may be nonspecific or of such low affinity that it would not be physiologically relevant. To try to determine if the high stoichiometry binding of $\text{Ti}(\text{L1})_3^{2-}$ was nonspecific, 0.01% Brij was included in reaction solutions. While the total number of bound metal complex molecules decreased, this decrease may have been facilitated by the precipitation of Ti(IV) species. When albumin samples are extensively dialyzed, only 1 equiv of complex remains bound even at low micromolar concentrations. The lower stoichiometry determined in these studies

(44) Fasman, G. D. *CRC Handbook of Biochemistry and Molecular Biology I*; CRC Press: Cleveland, 1975.

(45) *The Merck Index*; Budvari, S. Ed.; Merck & Co.: Rahway, NJ, 1989; p 3389.

(46) Comba, P.; Merbach, A. *Inorg. Chem.* **1987**, *26*, 1315–1323.

(47) Sommer, L. *Collect. Czech. Chem. Commun.* **1963**, *28*, 2102.

(48) Heller, G.; Schwarzenbach, G. *Helv. Chim. Acta* **1952**, *35*, 812.

could also be the result of titanium precipitation due to the lability of $\text{Ti}(\mathbf{L1})_3^{2-}$, especially during the extensive dialysis in metal complex-free and ligand-free buffer. Stoichiometric binding constants for the first three primary sites were determined by microequilibrium dialysis to be $K_1 = (2.05 \pm 0.34) \times 10^6 \text{ M}^{-1}$; $K_2 = (1.0 \pm 0.5) \times 10^5 \text{ M}^{-1}$; and $K_3 = (3.0 \pm 1.8) \times 10^5 \text{ M}^{-1}$. These values indicate that $\text{Ti}(\mathbf{L1})_3^{2-}$ binds with moderate affinity to albumin, which could be medically important.

The nature of the primary binding site of $\text{Ti}(\mathbf{L1})_3^{2-}$ was probed by competition studies. The precise location of this site was not identified. However, the complex does not bind to the primary sites of bilirubin, bromophenol blue, hemin, ibuprofen, or $\text{Ti}(\text{citrate})$. This result is partly unsurprising considering how much bigger this complex is relative to the typical organic ligands that bind to the protein.² An interesting aspect of this experiment is that two different forms of $\text{Ti}(\text{IV})$, the citrate and naphthalene-2,3-diolate complexes, bind to albumin in different sites. Citrate and naphthalene-2,3-diolate are chemically different types of ligands; the former is aliphatic and hydrophilic while the latter is aromatic and hydrophobic. This result suggests that ligands can be used to direct metals to bind to different sites in the protein, which may possibly facilitate transport to distinct targets. The primary site for the binding of $\text{Ti}(\mathbf{L1})_3^{2-}$ may be a hydrophobic surface site. A further competition study with bilirubin showed that while the complex can displace bilirubin at two surface sites on BSA, its affinity for this site (2.07×10^4) is weaker than its stoichiometric binding constants, suggesting these are not primary sites for the complex. An equilibrium dialysis study with the derivative complex $\text{Ti}(\mathbf{L2})_3^{5-}$ showed that while this complex does bind to BSA it displays significantly weaker affinity to the primary site, with one-fifth as much bound as $\text{Ti}(\mathbf{L1})_3^{2-}$ under the same conditions. The hydrophilic sulfonate moieties likely disrupt some of the hydrophobic interactions that stabilize the binding of $\text{Ti}(\mathbf{L1})_3^{2-}$. Also, the more highly charged complex may bind at another site.

Interaction of $\text{Ti}(\text{IV})(\mathbf{L1})_3^{2-}$ with HsTf and DNA. $\text{Ti}(\text{IV})$ catecholate-like complexes are normally thought to be too stable in aqueous solution to be able to deliver $\text{Ti}(\text{IV})$ to HsTf at pH 7.4. The aqueous speciation studies performed in this work suggest that $\text{Ti}(\text{IV})$ in the presence of $\mathbf{L1}$ are somewhat labile and can hydrolyze in the pH 7–10 range. But the complexes that are formed possess affinity constants that are higher than the $\text{Ti}(\text{IV})$ affinity of the two hard metal binding sites of HsTf ($\log K = 26.8$ and 25.7), making the metal exchange process thermodynamically unfavorable.¹³ From a kinetic perspective, $\text{Ti}(\mathbf{L1})_3^{2-}$ is also expected to be unable to deliver the metal ion to HsTf. It is easy to imagine that, even if favorable, the mechanism of exchange cannot be full dissociation of the ligands, followed by binding to HsTf, because aqueous $\text{Ti}(\text{IV})$ would precipitate. The character of the ligand is important for metal delivery to HsTf. If the metal is ligated by citrate, that ligand is far more flexible (it can go from tridentate to bidentate to even monodentate coordination relatively easily) and might have favorable interactions with the hydrophilic surface of the

protein. Citrate, when it coordinatively saturates $\text{Ti}(\text{IV})$, delivers $\text{Ti}(\text{IV})$ far more rapidly⁷ than does $\mathbf{L1}$. The naphthalenediolate ligands are bigger, inflexible, and hydrophobic. Our work with $\text{Ti}(\mathbf{L1})_3^{2-}$ has implications for $\text{Ti}(\text{IV})$ trafficking in serum and shows what factors are important in metal complexation design to target specifically albumin over transferrin for binding of a $\text{Ti}(\text{IV})$ species.

The nature of the $\text{Ti}(\mathbf{L1})_3^{2-}$ complex, with its large aromatic ligands, suggested that perhaps this complex could interact with DNA. A possible reaction mode is intercalation⁴² followed by metal ion facilitated hydrolysis, as has been suggested for other aromatic bioactive $\text{Ti}(\text{IV})$ complexes.⁴⁹ However, while the complex binds to DNA, the characteristics of this interaction are not indicative of intercalation. Importantly, the association does not promote hydrolysis of DNA.

Conclusions

$\text{Ti}(\text{IV})$ complexes of $\mathbf{L1}$ and $\mathbf{L2}$ were synthesized in this study. X-ray crystallographic, mass spectrometric, cyclic voltammetric, ^1H and ^{13}C NMR, FT-IR and fluorescence techniques were used to characterize these complexes. Spectropotentiometric titration studies were performed to determine the speciation of $\text{Ti}(\text{IV})$ in the aqueous environment of these ligands. At the micromolar concentrations examined, very stable complexes form that maintain the $\text{Ti}(\text{IV})$ soluble through at least pH 12.0. $\text{Ti}(\text{IV})$ hydrolysis occurs but only above pH 9.0. Four $\text{Ti}(\text{IV})$ species adequately represent the spectropotentiometric data, TiLH_0 , TiL_2H_0 , TiL_3H_0 , and $\text{TiL}_3\text{H}_{-1}$. The reduction potentials of the $\text{Ti}(\text{IV})$ tris(ligand) complexes are extremely negative suggesting that biological agents are unlikely to reduce the metal from $\text{Ti}(\text{IV})$ to $\text{Ti}(\text{III})$. At pH 7.4, the dominant species is TiL_3H_0 . The $\text{Ti}(\mathbf{L1})_3^{2-}$ version of the species binds with moderate affinity to multiple sites of BSA. The identity of its primary site is yet undetermined but is most likely a hydrophobic surface site. A weaker affinity at this site is observed for the $\mathbf{L2}$ version of the complex, most likely because of the hydrophilic sulfonate moiety. $\text{Ti}(\mathbf{L1})_3^{2-}$ binding to the primary site is quite stable. It remains bound to the site even after extensive dialysis. The complex is unable to deliver $\text{Ti}(\text{IV})$ to HsTf and though it can associate with DNA, the DNA bound complex does not display any cleavage activity. These results suggest mechanisms by which specific targeting of serum albumin for binding and transport of soluble $\text{Ti}(\text{IV})$ are possible.

Acknowledgment. We greatly appreciate Prof. Alanna Schepartz for use of her fluorimeter and Dr. Helmut Ernstberger for his help with cyclic voltammetry. We thank the Thomas Shortman Training, Scholarship, and Safety Fund for a fellowship (A.D.T.) and the American Cancer Society New England Division Research Scholar Grant for funding this work. We also thank the Yale College Dean's Research Fellowship and the Jacqueline M. and Donald L. Heywood

(49) Caruso, F.; Pettinari, C.; Marchetti, F.; Natanti, P.; Phillips, C.; Tanski, J.; Rossi, M. *Inorg. Chem.* **2007**, *46*, 7553–7560.

('50 B.S., '54 Ph.D.) Fellowship for the Physical Sciences for funding E.V.E.

Supporting Information Available: The syntheses of $K_2[Ti(L1)_3] \cdot 3H_2O$ (photo of the crystals and structure determination data) and $Cs_5[Ti(L2)_3] \cdot 2.5H_2O$ (preliminary structure). Details on $Ti(L1)_3^{2-}$ BSA competition binding studies. Electrospray mass

spectrometric, cyclic voltammogram, fluorescence data for Ti(IV) complexes of **L1** and **L2**. UV-vis difference titration of BSA into bromophenol blue and agarose gel of salmon sperm DNA in the presence and absence of $Ti(L1)_3^{2-}$. This material is available free of charge via the Internet at <http://pubs.acs.org>.

IC800529V